ePublishing

ΕΘΝΙΚΟ ΚΕΝΤΡΟ ΤΕΚΜΗΡΙΩΣΗΣ
EKT NATIONAL DOCUMENTATION CENTRE

HNPS Advances in Nuclear Physics

Vol 19 (2011)

HNPS2011

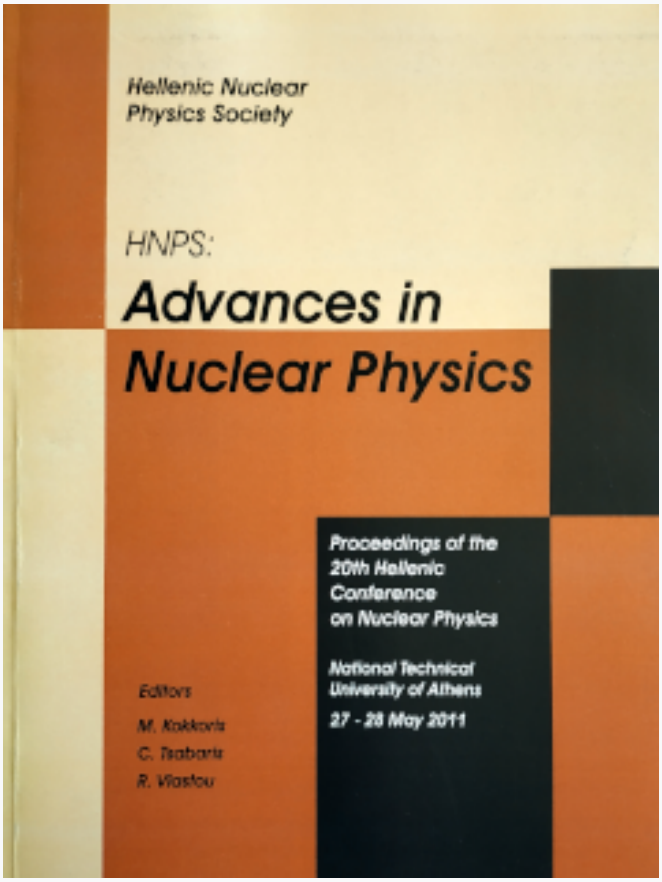

Lifetime Measurements at NCSR “Demokritos”

S. F. Ashley, M. Axiotis, V. Foteinou, S. Harrisopulos, T. Konstantinopoulos, A. Lagoyannis, T. J. Mertzimekis, G. Provatas

doi: 10.12681/hnps.2514

To cite this article:

Ashley, S. F., Axiotis, M., Foteinou, V., Harrisopulos, S., Konstantinopoulos, T., Lagoyannis, A., Mertzimekis, T. J., & Provatas, G. (2020). Lifetime Measurements at NCSR “Demokritos”. *HNPS Advances in Nuclear Physics*, *19*, 41–49. https://doi.org/10.12681/hnps.2514

https://epublishing.ekt.gr | **e-Publisher:** EKT | **Downloaded at:** 08/04/2026 03:52:41

Lifetime Measurements at NCSR "Demokritos"

S. F. Ashley, M. Axiotis, V. Foteinou, S. Harissopulos, T. Konstantinopoulos, A. Lagoyannis, T. J. Mertzimekis, G. Provatas

Institute of Nuclear Physics, Tandem Accelerator Laboratory, NCSR "Demokritos", Aghia Paraskevi, Athens GR.-153.10, Greece

Abstract

Proof-of-principle inelastic proton scattering measurements have been performed at NCSR "Demokritos". Excited states in ^{64}Zn and ^{92}Mo were populated using the (p,p$'\gamma$) reaction with E(p) = 7 MeV. The reaction γ rays were detected using four HPGe detectors at eight separate angles, with respect to the beam-axis. From Doppler-shift attenuation of the γ rays, lifetimes for eight excited states in ^{64}Zn and for the $I^{\pi} = 2_2^+$ and 2_3^+ states in ^{92}Mo were deduced. The lifetimes measured in ^{92}Mo are in good agreement with adopted values whereas the lifetimes measured in ^{64}Zn are typically longer than the literature values. Development of the experimental set-up and potential novel physics cases where this reaction could be used are briefly discussed.

1 Introduction

By determining the lifetimes of excited states in atomic nuclei, one can gain a significant insight into the nature behind the modes of excitation which atomic nuclei purvey. This insight arises as there is direct correspondence between the mean lifetime of the excited state and the reduced matrix elements between transitions from this excited nuclear state to lower-energy states. Typically, "prompt" transitions within atomic nuclei range from femtoseconds up to a nanosecond. Within this range, the lifetimes can be extracted by measuring certain properties of the γ-ray de-excitation. For sub-picosecond lifetimes, one may deduce the lifetime from the peak-width if it is a resonant excitation (e.g. from an excited state populated using Nuclear Resonance Fluoresence [1]), from the shift in the centroid position from the de-excitation of an excited state populated by compound nuclear reactions or from the lineshape from

the de-excitation of excited states populated by fusion-evaporation reactions [2].

By using low-energy inelastic nucleon scattering [3], one can populate and deduce the properties (including the lifetime) of non-yrast excited states, with angular momentum ranging from zero to six. This allows for the study of collective excitations in atomic nuclei, such as those associated with critical-point symmetries [4,5], and also for the search of other exotic nuclear phenomena such as mixed-symmetry states [6]. Furthermore, for nuclei up to A$\sim$100, information on the reduced matrix elements allows for a robust test of effective interactions that are used in shell-model calculations [7].

This paper will present details of two proof-of-principle inelastic proton scattering experiments performed at NCSR "Demokritos". These measurements consisted of determining the lifetimes of excited states in ^{64}Zn and ^{92}Mo via the (p,p$'\gamma$) reaction, which have been previously determined by alternative and complementary reactions.

2 Experimental Technique and Data Analysis

To test whether sub-picosecond excited state lifetimes could be reliably extracted via the (p,p$'\gamma$) reaction, two proof-of-principle measurements were performed at the Tandem Accelerator Laboratory at NCSR "Demokritos" to extract the lifetimes of excited states in ^{64}Zn and ^{92}Mo. For both measurements, protons were accelerated by the T11/25 tandem Van de Graaff accelerator to an energy of E(p) = 7 MeV with a typical intensity of I(p) $\approx$ 10 - 20 pnA. For the ^{64}Zn measurement, a 3.5(3) mg/cm^2 self-supporting target was used. For the ^{92}Mo measurement, a 5.0(5) mg/cm^2 self-supporting target was used. The target thicknesses were deduced using RBS in a separate experiment prior to these measurements. Reaction γ rays were detected using three HPGe detectors (with 100% relative efficiency) from the "ADAKOM" pool and a fourth HPGe detector (with 80% relative efficiency) from INP, NCSR "Demokritos". The HPGe detectors were mounted at a distance of 32(2) cm, on a rotating table which allowed reaction γ rays to be measured at 0°, 15°, 40°, 55°, 90°, 105°, 150° and 165°, with respect to the beam-axis. Signals from the HPGe detectors were amplified using four CANBERRA 2022 modules with a shaping-time of 4 μs. The data acquisition system comprised of two FASTCom 7072 dual 8k ADC modules coupled to a FASTCom SPA3 multichannel analyzer. To minimise possible drifts and shifts within the electronics, data were recorded in runs lasting no longer than 30 minutes. To monitor for drifts in the electronics, a ^{137}Cs and ^{60}Co were placed close to the target position. Also, activation spectra were recorded for 6 minutes between each run. Calibration and non-linearity (up to 1.5 MeV) of the electronics was performed with an

IAEA calibrated ^{152}Eu source. For the ^{64}Zn measurement, twenty minutes of data per angle were recorded, whereas for ^{92}Mo, two and a half hours of data per angle were recorded. Spectra were analysed off-line using the computer program TV [8].

The data analysis comprised of determining the centroid positions of various reaction γ rays that could be resolved for each detector angle. As the centroid of the Doppler-shifted γ ray is represented by Equation 1,

$$E_\gamma(\theta) = E_\gamma(90^\circ)[1 + F(\tau)\,\beta\,\cos(\theta)] \tag{1}$$

where E_γ denotes the γ-ray energy, θ denotes the polar angle of the detector with respect to the beam-axis, $F(\tau)$ is attenuation factor which is a function of the mean lifetime of the excited state (τ), and β is the recoil velocity (as a fraction of the speed of light, c) of the target nucleus in the centre of mass frame of reference. For the (p,p$'\gamma$) reaction, β is described in Equation 2 [9],

$$\beta = \frac{v_{cm}}{c} = 0.04635\frac{A_P}{A_P + A_T}\sqrt{\frac{E_P}{A_P}} \tag{2}$$

where A_P and A_T are the masses of the projectile and target, respectively, in amu, and E_P is the energy of the projectile in MeV. By plotting, E_γ vs. $\cos(\theta)$, one extracts the experimental $F(\tau)$ value ($F(\tau)_{EXP}$). This $F(\tau)_{EXP}$ value is compared to theoretical $F(\tau)_{THE}$ values obtained using Winterbon's formalism [9]. This analytical method has been applied for (n,n$'\gamma$) reactions [10] and an identical approach has been adopted for this work. In a nutshell, Winterbon's formalism describes the slowing down process of a recoiling nucleus in an infinite, isotropic, homogenous medium. This yields an attenuation factor described by Equation 3 (as derived in Ref. [10]).

$$\begin{aligned}\langle F(\tau)v_{cm}.\mathbf{n}\rangle = v_{cm}\cos\theta_\gamma\Big[&F(\tau, v_{cm}) + F'(\tau, v_{cm})\,v_{cm} \\ &\times\left(\frac{3}{5} - \frac{8z(A_T+1)}{15A_T} - \frac{z^2(A_T+1)^2}{15A_T^2}\right)\Big]\end{aligned} \tag{3}$$

where $F(\tau, v_{cm})$ is analytically determined using the computer code V1PGM [11], $F'(\tau, v_{cm})$ is the derivative of $F(\tau)$ value for lower and upper bounds of the recoil velocity (which is approximately linear in the range from $0.8\,v_{cm}$ to $1.2\,v_{cm}$) and $z = E_{lev}/E_P$. The $F'(\tau, v_{cm})$ term is incorporated to account for the nuclear stopping term and shifts the decay curve to longer lifetimes.

I_i^π	E_x (keV)*	$I_i^\pi \rightarrow I_f^\pi$	E_γ (keV)*	$F(\tau)_{EXP}$	τ (fs) [a]	τ (fs) [b]	τ (fs) [c]
2_4^+	3005.7	$2_4^+ \rightarrow 2_2^+$	1206.2	0.30(2)	128^{+19}_{-15}	115(30)	175(21)
1^+	3186.8	$1^+ \rightarrow 0_2^+$	1276.5	0.31(4)	122^{+29}_{-22}	375(185)	165^{+37}_{-28}
1	3262.0	$1 \rightarrow 2_1^+$	2270.4	0.56(2)	46(3)	60(20)	63(5)
1^+	3366.0	$1^+ \rightarrow 0_1^+$	3365.9	0.59(4)	41(8)	33(11)	57(9)
1^+	3425.2	$1^+ \rightarrow 2_1^+$	1625.7	0.24(9)	172^{+139}_{-66}	45(10)	225^{+145}_{-85}
$(2,3)$	3458.6	$(2,3) \rightarrow 2_2^+$	1659.2	0.10(3)	490^{+180}_{-110}	340(90)	630^{230}_{-145}
$(2,3)$	3458.6	$(2,3) \rightarrow 2_1^+$	2467.1	0.05(2)	1230^{+1020}_{-410}	340(90)	1590^{+1340}_{-550}
1^-	3701.4	$1^- \rightarrow 0_1^+$	3701.3	0.60(3)	39(6)	-	53(6)
$(0^+ - 4^+)$	3718.4	$(0^+ - 4^+) \rightarrow 2_1^+$	2726.8	0.52(2)	54(6)	45(15)	72(6)

Table 1
Results of the ^{64}Zn(p,p′γ) experiment with E(p) = 7 MeV. * Values adopted from Ref. [12]. [a] Denotes lifetimes measured in this work without correction for level feeding. [b] Denotes lifetimes reported from Refs. [13,14]. [c] Denotes lifetimes measured in this work with correction for level feeding.

3 Results

3.1 ^{64}*Zn*

The left panel of Figure 1 shows the recorded γ-ray spectrum for the ^{64}Zn(p,p′γ) reaction with E(p) = 7 MeV in the 80% HPGe detector at 90°. This particular spectrum was accumulated over twenty minutes of beam on target. In total, nine transitions produced $F(\tau)$ plots which could be satisfactorily fitted by linear regression and the reaction γ-rays for these transitions are listed in Column 4 of Table 1. Plots of E_γ vs. cos(θ), with the deduced $F(\tau)_{EXP}$ values are shown in the right panel of Figure 1. The corresponding comparison between these $F(\tau)_{EXP}$ values and $F(\tau)_{THE}$ curves, including the correction for level feeding shown in Equation 3 are shown in the left panel of Figure 2, along with the extracted lifetime. It should be noted that due to uncertainties in the stopping-powers used within the computer code V1PGM, the errors in the deduced lifetime, presented in Figure 2, need to be increased by 10%. These corrected lifetime values are shown in Column 8 of Table 1. In the right panel of Figure 2, a comparison between $F(\tau)_{EXP}$ values and $F(\tau)_{THE}$ curves, without the aforementioned correction for level feeding is presented, with the corresponding lifetimes (corrected for associated uncertainties in the stopping-powers) being shown in Column 6 of Table 1.

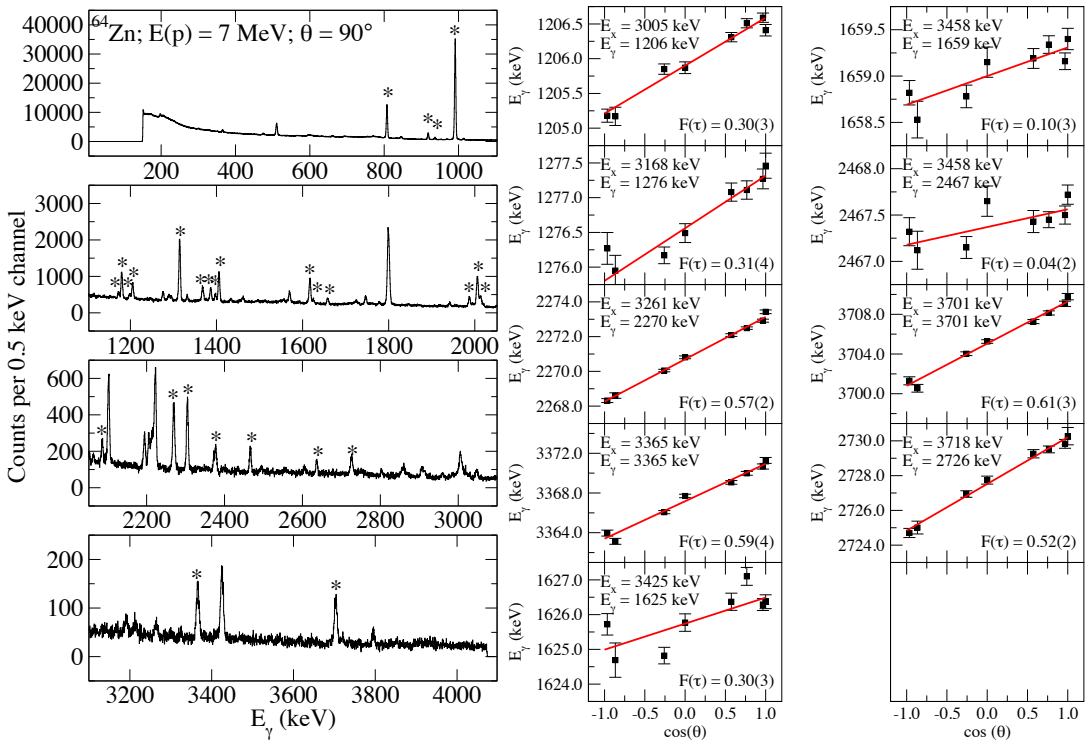

Fig. 1. Left: Recorded γ-ray spectrum from the ^{64}Zn(p,p$'\gamma$) reaction with E(p) = 7 MeV. Asterisked transitions were reaction γ rays that were analyzed in this work. Right: Plots of $E_\gamma$vs. cos(θ), with deduced $F(\tau)_{EXP}$ value for nine transitions in ^{64}Zn.

3.2 ^{92}*Mo*

Figure 3 shows the γ-ray spectrum recorded over a time period of two and a half hours in the 80% HPGe detector at 90° for the ^{92}Mo(p,p$'\gamma$) reaction with E(p) = 7 MeV. The notable γ rays seen in this spectrum are the 1510-keV $I^\pi = 2_1^+ \rightarrow 0_1^+$ transition, 1582-keV $I^\pi = 2_2^+ \rightarrow 2_1^+$ transition, 2032-keV $I^\pi = 2_3^+ \rightarrow 2_1^+$ transition and 3094-keV $I^\pi = 2_2^+ \rightarrow 0_1^+$ transition. Plots of E_γ vs. cos(θ), with the deduced $F(\tau)_{EXP}$ values are shown in the top portion of Figure 4. The lower portion of Figure 4 shows the comparison between the extracted $F(\tau)_{EXP}$ values and $F(\tau)_{THE}$ curves, inclusive of the correction for level feeding shown in Equation 3. In similar fashion to the analysis of ^{64}Zn, the errors on the lifetimes presented in Figure 4 are inflated by 10% and are reported in Column 5 of Table 2.

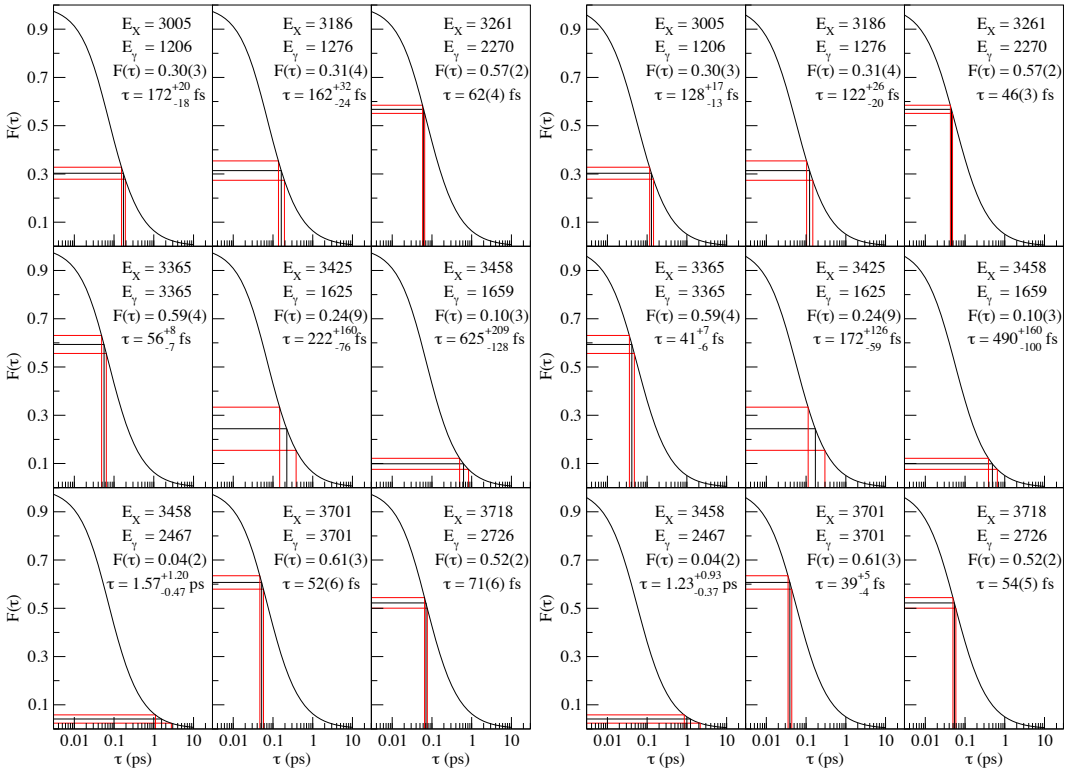

Fig. 2. Comparison of experimental and theoretical $F(\tau)$ values. Left: Theoretical decay curves including level feeding correction. Right: Theoretical decay curves without level feeding correction.

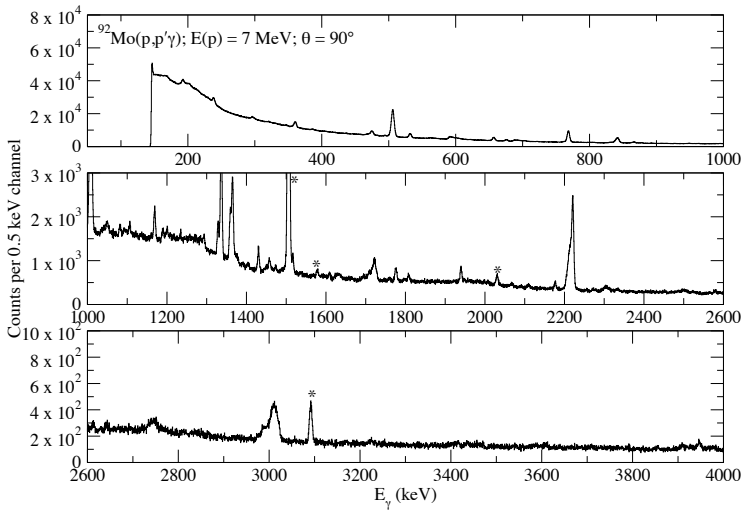

Fig. 3. Recorded γ-ray spectrum from the ^{92}Mo(p,p$'\gamma$) reaction with $E(p) = 7$ MeV. Asterisked transitions were reaction γ rays that were analyzed in this work.

4 Discussion

4.1 ^{64}Zn

A total of thirty transitions were analyzed up to a level energy of $E_x \sim 4$ MeV. Only nine could be satisfactorily fitted with a linear regression to attain an

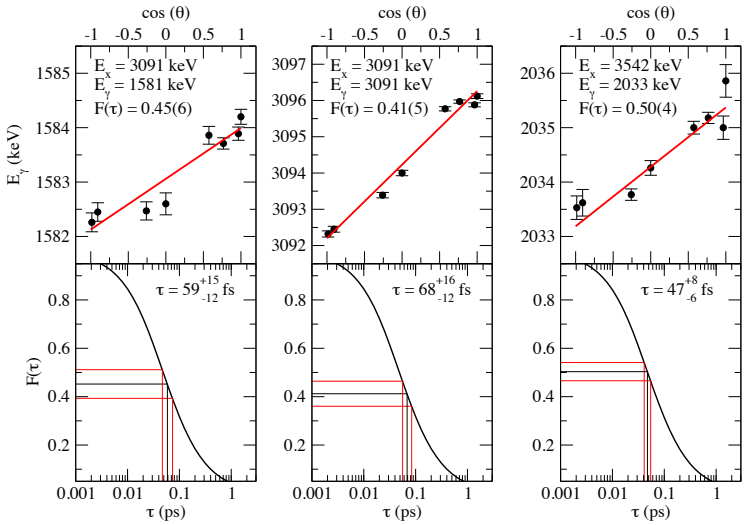

Fig. 4. Upper: Plots of E_γ vs. cos(θ) for the 1582 keV, 2032 keV and 3094 keV transitions in ^{92}Mo. Lower: Corresponding extracted lifetimes from theoretical and experimental $F(\tau)$ values.

I_i^π	E_x (keV)*	$I_i^\pi \rightarrow I_f^\pi$	E_γ (keV)*	$F(\tau)_{EXP}$	τ (fs) [SFA]	τ (fs) [ENSDF]
2_2^+	3094	$2_2^+ \rightarrow 2_1^+$	1582	0.45(6)	59^{+17}_{-13}	46.2(30)
		$2_2^+ \rightarrow 0_1^+$	3094	0.50(4)	47^{+18}_{-13}	46.2(30)
2_3^+	3584	$2_3^+ \rightarrow 2_1^+$	2032	0.41(5)	68^{+9}_{-7}	51(23)

Table 2
Results of the ^{92}Mo(p,p$'\gamma$) experiment with E(p) = 7 MeV. * Values adopted from Ref. [15]. [SFA] denotes lifetimes deduced in this work. [ENSDF] denotes evaluated lifetimes presented in [15].

$F(\tau)_{EXP}$ value. This is attributed to having four separate detection systems which would need to have their non-linearities accounted for to a larger energy range to minimize systematic deviations between these systems. Furthermore, a runshift calibration which can be used over a larger region of the ADC is also desired. In both cases where the level feeding correction (outlined in Equation 3) was applied and ignored, the deduced lifetimes were systematically too long. Therefore, a re-analysis of the $F(\tau)_{EXP}$ values presented in Refs. [13,14] with Winterbon's formalism used in this work is required to compare the $F(\tau)_{EXP}$ are.

4.2 ^{92}Mo

In total, three separate linear regressions were applied to the 1583 keV, 2032 keV and 3094 keV transitions and $F(\tau)_{EXP}$ values of 0.45(6), 0.41(5) and 0.60(4)

were deduced respectively, and are in good agreement with $F(\tau)$ values of 0.470(114), 0.310(107) and 0.580(65) presented in Ref. [16]. The 1510 keV transition could be fitted though it would have been intractable to correct for the lifetimes of the excited states feeding this low-lying $I^{\pi} = 2_1^+$ state. As seen in Columns 6 and 7 of Table 2, there is good agreement between the lifetimes measured in this work and the evaluated lifetimes in Ref. [15].

4.3 Future Work

As indicated in Section 4.1, large deviations occur between accounting for and ignoring level-feeding and that experimental data obtained near the reaction threshold exist within these two limits. Due to the Coulomb-barrier, the energy of the incident proton is well above the threshold will be needed to satisfactorily populate the states and so an extension of Belgya's formalism (Equation 3) may be required and this can be investigated with TALYS [17]. Also, the need for accurate energy and efficiency calculations are required and so the utilisation of ^{226}Ra and ^{88}Y is needed. Finally, the implementation of particle-γ coincidences is desired to clean up the γ-ray spectra and to allow more straight-forward determination of the level scheme.

5 Conclusion

Proof of principle experiments have been performed to determine the lifetime of sub-picosecond states within ^{64}Zn and ^{92}Mo via the Doppler-shift attenuation method. For ^{64}Zn, nine individual lifetimes were determined and were systematically too long to lifetimes presented in Refs. [13,14]. Further work to refine this formalism and to apply this formalism to other light-ion compound-nucleus reactions is required. For ^{92}Mo, the deduced $F(\tau)$ values were in agreement with those reported in Ref. [16], the corresponding lifetimes are within agreement by those reported in Ref. [15].

References

[1] U. Kneissl, H. H. Pitz and A. Zilges, Progr. Part. Nucl. Phys. **37** (1996) 349.

[2] P. J. Nolan and J. F. Sharpey-Schafer, Rep. Progr. Phys. **42** (1979) 1.

[3] E. Sheldon and D. M. van Patter, Rev. Mod. Phys. **38** (1966) 143.

[4] F. Iachello, Phys. Rev. Lett. **85** (2000) 3580.

[5] F. Iachello, Phys. Rev. Lett. **87** (2001) 052502.

[6] N. Pietralla, P. von Brentano and A. F. Lisetskiy, Progr. Part. Nucl. Phys. **60** (2008) 225.

[7] E. Caurier, G. Martínez-Pinedo, F. Nowacki, A. Poves and A. P. Zuker, Rev. Mod. Phys. **77** (2005) 427.

[8] J. Theuerkauf, et al., Tv, unpublished, "TV", unpublished, http://www.ikp.uni-koeln.de/∼fitz (1993).

[9] K. B. Winterbon, "Calculation of Doppler-Shift Attenuation", AECL Report 4829.

[10] T. Belgya, G. Molnár and S. W. Yates, Nucl. Phys. A **607** (1996) 43.

[11] T. Belgya, B. Fazekas and N. Warr, Computer Code: V1PGM; University of Kentucky, unpublished.

[12] B. Singh, Nucl. Data Sheets **108** (2007) 197.

[13] D. N. Simister et al., J. Phys. G. **4** (1978) 111.

[14] D. N. Simister et al., J. Phys. G. **6** (1980) 81.

[15] C. M. Baglin, Nucl. Data Sheets **91** (2000) 423.

[16] C. T. Papadopoulos et al., Nucl. Phys. A **254** (1975) 93.

[17] A. J. Koning, S. Hilaire and M. C. Duijvestijn, "TALYS-1.0", Proc. Int. Conf. on Nucl. Data for Sci. and Tech., (2008) 211.